Textile & Leather Review

ISSN 2623-6281| www.tlr-journal.com | 10.31881/TLR

Dynamic Path Planning Model for Mine Water Inrush Based on Breadth-First Search and Time-Extended Dijkstra Algorithm

Jin Deng, Wen Li, Shujie Liu, Shiting Wang

How to cite: Deng J, Li W, Liu S, Wang S. Dynamic Path Planning Model for Mine Water Inrush Based on Breadth-First Search and Time-Extended Dijkstra Algorithm. Textile & Leather Review. 2026; 9:1935-1957. https://doi.org/10.31881/TLR.2026.1935

How to link: https://doi.org/10.31881/TLR.2026.1935

Published: 25 April 2026

Dynamic Path Planning Model for Mine Water Inrush Based on Breadth-First Search and Time-Extended Dijkstra Algorithm

Jin Deng[1]*, Wen Li[2], Shujie Liu[2], Shiting Wang[2]

[1]Basic Courses Department, Hunan College of Information, Changsha 410200, Hunan, China

[2]School of Software Engineering, Hunan College of Information, Changsha 410200, Hunan, China

*dadjy_hd@163.com

Article

https://doi.org/10.31881/TLR.2026.1935

Published 25 April 2026

ABSTRACT

This study constructs a series of models for water flow propagation in mine tunnel water inrushes and dynamic escape path planning for miners, aiming to provide reference escape strategies for mine water disasters. For single-point water outburst scenarios, the study abstracts the roadway network as a graph structure. Employing a breadth-first search algorithm, it calculates the time of first water arrival at endpoints and the time of roadway flooding, incorporating spatial parameters and initial outburst flow rates. For optimal miner escape route planning, the study introduces dynamic velocity constraints based on water depth: 4 m/s in dry conditions, 2 m/s downstream and 1 m/s upstream in low water, with high water levels prohibiting movement. The defined velocity constraints under different water depths provide essential ergonomic performance metrics for the development of miners' protective clothing in hydraulic environments. The model employs a time-extended Dijkstra algorithm to search for the shortest total escape time path. Building upon this foundation, the model is extended to predict flow superposition in delayed dual-source water inrushes. By applying time axis shifts, selecting minimum arrival times, and superimposing flow rates, it calculates flow states under dual-source interactions, enabling dynamic simulation of multi-source inrush systems. Finally, integrating dual-source flow results with the time-varying Dijkstra algorithm, the model plans optimal miner escape routes during delayed dual-source water inrushes. This study offers a theoretical framework for integrating wearable safety systems into intelligent mine disaster mitigation.

KEYWORDS

protective clothing performance, breadth-first search, time-extended dijkstra algorithm, water flow propagation model

INTRODUCTION

Mine water disasters pose a significant threat to mining safety, often resulting in substantial casualties and economic losses[1, 2]. Therefore, rapidly simulating water flow propagation and determining optimal miner escape routes is critical. In the context of modern mining safety, the synergy between escape algorithms and high-performance individual protective equipment, such as industrial textile-based safety suits, is increasingly vital for ensuring miner biosafety. Mine tunnel systems typically form three-dimensional networks with intersecting passages. Water flow propagation is influenced by spatial parameters of tunnel cross-sections, inflow rates at water inrush points, and tunnel elevation profiles. The core objective of this study is to establish a water flow propagation model for mine water inrushes and to plan optimal miner escape routes based on dynamic water flow conditions, providing actionable evacuation strategies for mine water disasters. While prior studies have addressed water flow propagation and path planning, they struggle to simultaneously handle complex scenarios involving multiple delayed water inrush sources, flow accumulation, and dynamic speed variations with time constraints during miner evacuation. The innovations of this research are: First, systematically constructing a water flow propagation prediction model for a single inrush point based on the breadth-first search (BFS) algorithm, strictly adhering to the principle that “water flows downward” to address flow diversion issues. Second, it innovatively converts the physical constraints imposed by water flow on miners into dynamic passage times, integrating these with a time-extended Dijkstra algorithm to solve the dynamic exploration of shortest escape time paths. Third, it extends the single-source model to a delayed dual-source water inrush superposition model, addressing changing water flow states under complex water inrush disasters through time axis shifting and flow superposition. The research approach in this section is divided into four phases: First, establish a BFS algorithm model to calculate water arrival and inundation times under single-source water inrushes. Second, construct a time-extended Dijkstra algorithm model to plan miner escape routes under single-source scenarios. Third, extend the single-source model to dual-source water inrushes, addressing delay and flow superposition issues. Finally, based on dual-source results, re-plan optimal miner escape routes using a time-varying Dijkstra algorithm[3].

MODEL ESTABLISHMENT AND SOLUTION

Establishment and Solution of Water Flow Spread Model for Single Water Inrush Point

Data Preprocessing

In the Mine 1 case, all z-coordinates being 10.00m makes it a special planar diffusion benchmark. This contrasts with Mine 2's 3D topology to jointly validate the model's robustness in handling ‘horizontal-vertical’ hybrid networks. The data is from www.mcm.edu.cn. Python is first used to read the data of roadway and endpoint coordinates. Through steps such as missing value detection and outlier identification, it is confirmed that the data is free of abnormalities. All z-coordinates of roadways and endpoints are the same (10.00m), so only the horizontal and vertical coordinates of the roadways are considered. Combined with the position coordinates of the water inrush point A1 (5349.03, 4931.90, 10.00), Python software is used to draw a network diagram of the mine roadways and the water inrush point A1 (Figure 1):

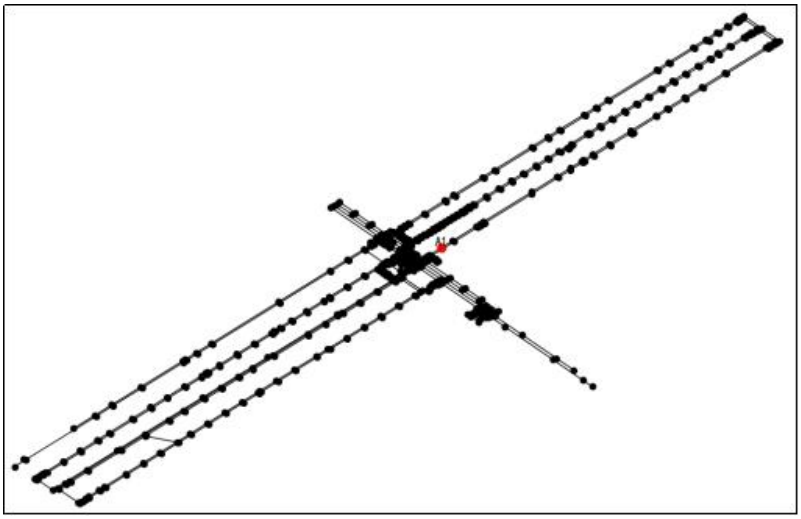

Figure 1. Schematic diagram of the mine roadway network and water inrush point A1

The figure 1 above presents the topological structure of the mine roadway network from a planar perspective, where all black dots are roadway endpoints, and the line segments connecting the endpoints are the connecting lines of the midpoints of the roadway bottoms. Since the vertical coordinates of all roadway endpoints are the same, the roadways in the mine are all horizontal, with no "downward roadways" or "upward roadways"[4,5].

By observing the data, it is found that the water inrush point A1 is not on the line connecting the mine roadway endpoints (Figure 2). Through comparative analysis of the position information between A1 and the nearest adjacent roadway, it is found that A1 is located within the roadway P0351-P0358, and the water flows horizontally around from here.

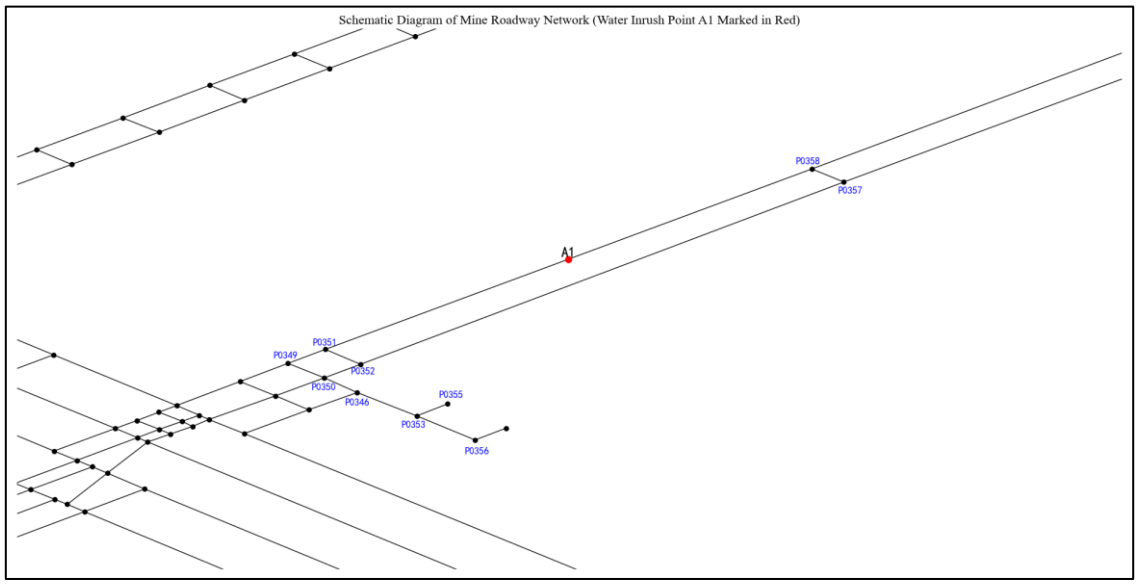

Figure 2. Schematic diagram of the relative position between the water inrush point A1 and the nearest adjacent roadway

Model Idea and Analysis

This model employs the BFS algorithm for calculating water inrush propagation, primarily based on the simplified assumption of consistent tunnel parameters. Although Dijkstra demonstrates greater robustness in handling networks with variable flow velocities, BFS effectively completes topological traversal in this model since all tunnels are initially treated as having similar hydraulic properties. Future research may incorporate the Dijkstra framework to accommodate more complex heterogeneous flow velocity scenarios.

Water Inrush Flow Propagation Model Based on Breadth-First Search (BFS) Algorithm

Considering that the propagation process of water inrush in mine roadways starts from the water inrush point and flows to adjacent nodes along the connecting line of the midpoints of the roadway bottoms, this process is similar to the point-line traversal structure of a directed graph[6]. Therefore, the BFS (Breadth-First Search) algorithm is selected, and the specific steps of the algorithm are as follows:

Step 1: Add the water inrush point to the initial endpoint queue M;

Step 2: Repeat Step 3 until the endpoint queue M is empty;

Step 3: Take out the head roadway endpoint from the queue M, find the unvisited endpoints connected to this endpoint, mark them, add them to the queue M, and delete the visited endpoints from the queue.

The algorithm flow chart is shown in Figure 3:

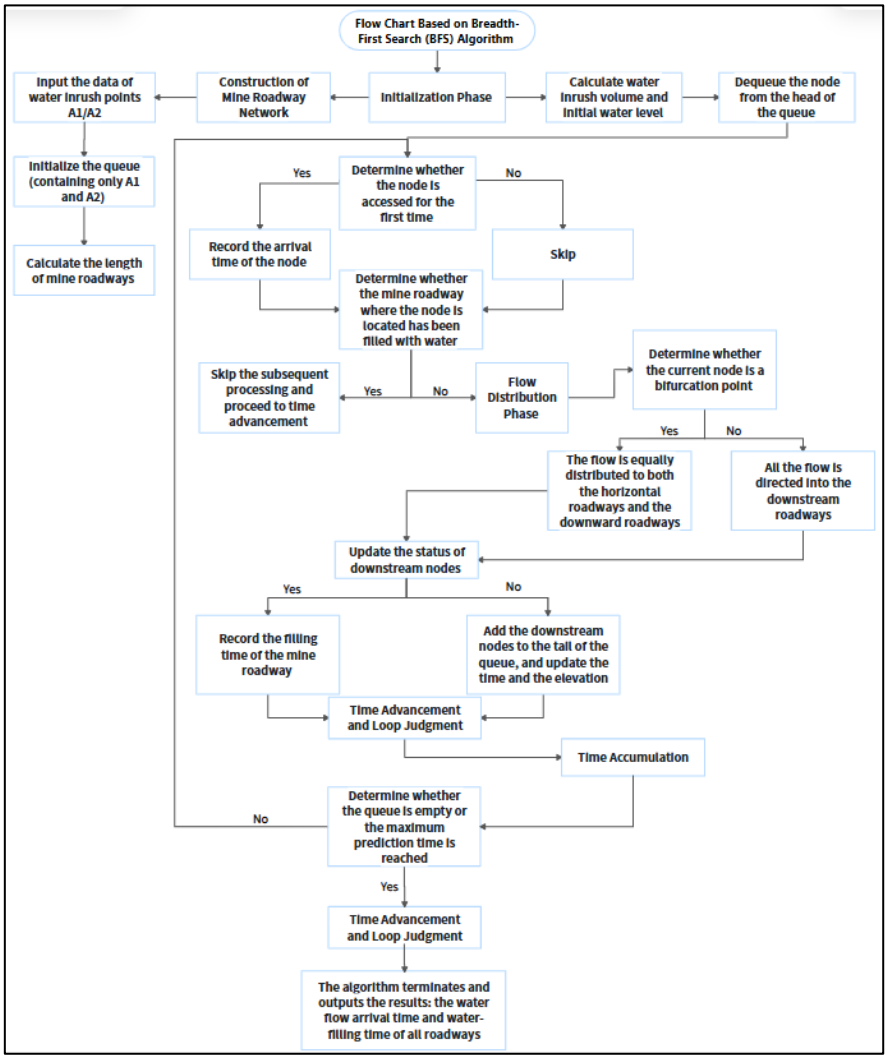

Figure 3. Schematic diagram of the algorithm flow

Model Solution

Given that the cross-sectional width of the roadway $l_0=4\ \mathrm{m}$ and the initial water level of the water inrush $h_0=0.1\ \mathrm{m}$, the cross-sectional area s_0 of the water flow when the water inrush point just erupts can be calculated as[7,8]:

$$s_0 = l_0 \cdot h_0 = 0.4\ \mathrm{m}^2 \tag{1}$$

Since the z-coordinates of all roadway endpoints in the mine are the same, only the planar distance is considered. According to the distance formula between two points, the length of the roadway P_iP_j is:

$$L_{ij} = \sqrt{(x_i - x_j)^2 + (y_i - y_j)^2} \tag{2}$$

where (x_i, y_i) are the coordinates of the endpoint P_i.

The length of each roadway is calculated with Python, and the specific results are detailed in "Roadway Length Calculation Results.xlsx" in the supporting materials.

Then, the water flow volume propagating in the roadway is:

$$Q_{\text{Propagating Water Volume}} = s_0 \cdot L_{ij} \tag{3}$$

Given that the volumetric flow rate at the water inrush point is $Q_{\text{Inrush}} = 30\ \mathrm{m}^3/\mathrm{min}$, the time for the water inrush to first propagate to the roadway endpoint P_j is:

$$t_{\text{Arrival}}(P_j) = \frac{Q_{\text{Propagating Water Volume}}}{Q_{\text{Inrush}}} = \frac{s_0 \cdot L_{ij}}{Q_{\text{Inrush}}} \tag{4}$$

Since the cross-sectional height of the roadway $l_1 = 3\ \mathrm{m}$, the cross-sectional area of the roadway is $s_{\text{Roadway}} = l_0 \cdot l_1 = 4 \times 3 = 12\ \mathrm{m}^2$.

The water flow volume when the roadway is full of water is:

$$Q_{\text{Full Water Volume}} = s_{\text{Roadway}} \cdot L_{ij} \tag{5}$$

Thus, the time when the roadway P_iP_j is full of water is:

$$t_{\text{Full}}(P_iP_j) = \frac{Q_{\text{Full Water Volume}}}{Q_{\text{Inrush}}} = \frac{s_{\text{Roadway}} \cdot L_{ij}}{Q_{\text{Inrush}}} \tag{6}$$

Starting from the water inrush point A1, the BFS algorithm is used to traverse all endpoints and line segments of the mine roadways. With Python software, the water flow arrival time at each endpoint and the full water time of each roadway in the mine are obtained.

The first 4 and last 4 endpoint water flow arrival times and roadway full water times are listed in Table 1:

Table 1. Water flow arrival times at some roadway endpoints and full water times of roadways

Endpoint Number	Water Flow Arrival Time (minutes)	Roadway Number	Full Water Time (minutes)
P0351	2.64	H0964	46.36
P0358	2.64	H0391	50.30
P0357	3.00	H0389	51.59
P0349	3.05	H0397	51.71
...	...	...	...
P0560	94.65	H0969	Unfillable
P0083	96.06	H0972	Unfillable
P0405	96.41	H0973	Unfillable
P0082	98.64	H0975	Unfillable

Since drainage mechanisms were not discussed and a computational cutoff time was set, ‘unfillable’ indicates that the roadway had not reached saturation within the effective observation window period for miner evacuation due to flow distribution (e.g., diversion at P0095).

Analysis of the above table shows:

(1) The water flow arrival times at the roadway endpoints P0351 and P0358 are both 2.64 minutes. The roadway corresponding to these two endpoints is numbered H0399, and the full water time of the roadway is "Unfillable". This is because the water inrush point A1 is exactly located within the roadway H0399, and

the projection of A1 on the roadway line is exactly the midpoint of the endpoints P0351 and P0358. Therefore, the time for the water flow to reach these two endpoints for the first time is the same, which is consistent with the actual situation.

(2) For the endpoints P0091 and P0095, the water flow arrival times are 11.09 minutes and 11.76 minutes respectively, corresponding to the roadway H0975, but the full water time of this roadway is also "Unfillable". This is because P0095 is the intersection of the roadways H0975, H0083, and H0092. When the water flow reaches here, it will be evenly divided, which also causes the roadway to be unfillable, consistent with the actual situation.

(3) For the roadway H0069, since it is the farthest from the water inrush point, its full water time is the longest.

Analysis of the Water Flow Propagation Model in Mine 2 (A2)

Similarly, a network diagram of the roadway endpoints and the water inrush point A2 (4143.12, 4376.28, 6.33)is drawn (Figure 4):

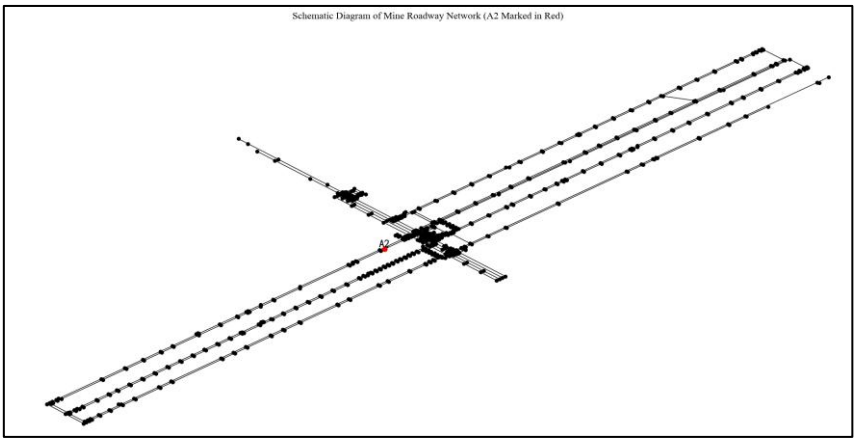

Figure 4. Schematic diagram of the mine roadway network (A2 marked in red)

The position coordinates of each roadway show that the z-coordinates of their endpoints are different. Therefore, in three-dimensional space, there are differences between high and low roadways. However, the problem statement clearly states that during water flow propagation, the water only diverges to horizontal and downward roadways[9,10]. Therefore, it is considered that during the water flow propagation process, the water cannot reach the high roadways[11,12].

Similar to the idea, the water flow volume during propagation and the water flow volume when the roadway is full of water are obtained based on the following two formulas.

Starting from the water inrush point A2, the BFS algorithm is also used, and Python is used to obtain the water flow arrival time at each endpoint and the full water time of each roadway in the mine. Some data are shown in Table 2:

Table 2. Water flow arrival times at endpoints and full water times of roadways

Endpoint Number	Water Flow Arrival Time (minutes)	Roadway Number	Full Water Time (minutes)
P0358	0.86	H0964	22.72
P0357	1.23	H0966	51.09
P0000	Unreachable	H0000	Unfillable
P0001	Unreachable	H0001	Unfillable

Nodes labeled ‘Unreachable’ in Table 2 (e.g., P0000) cannot be reached due to elevation constraints imposed by the principle that water flows downward, not because of network structural disconnectivity. This validates the model's logical correctness in handling 3D topology.

Analysis of the above table shows:

(1) The water flow arrival time at the roadway endpoint P0357 is the shortest (0.86 minutes), followed by P0358 (1.23 minutes). This is because the roadway where the endpoints P0357-P0358 are located is the closest to the A2 water inrush point, with the corresponding roadway number H0964, and the full water time of this roadway is also the shortest (22.72 minutes). This is because the roadway H0964 is the lowest in geographical location. As time goes by, this roadway must be full of water before the water can propagate to adjacent roadways, which is consistent with the actual situation[13].

(2) The water flow cannot reach the endpoints P0000 and P0001, which correspond to the roadway number H0000. At this time, the roadway cannot be filled with water, which is consistent with the actual data.

In summary, the water flow propagation model established has a good effect.

Model Result Analysis

The calculation results of the two annexes show that the flow distribution is uniform with small differences among branch flows; the flow distribution is highly uneven, mainly concentrated in the downstream roadways. This reveals the fundamental impact of elevation constraints on mine water inrush disasters. The model not only provides a more realistic prediction of water flow diffusion but also quantifies the existence and scope of topological safety zones for the first time, providing a new theoretical basis and practical guidance for mine water disaster prevention and control. These differentiated analysis results prove that mine water inrush emergency plans must consider the elevation characteristics of specific roadway networks and cannot simply apply planar diffusion models[14,15].

Miner Escape Path Planning Under Single Water Inrush Point Conditions

Model Idea and Analysis

The physical constraints to be considered include: water flow only propagates in downward/parallel roadways; wading passage is allowed when the water level in the roadway is ≤ 0.3m; wading passage is not recommended when the water level > 0.3m. Miners' movement speed is affected by the water flow (4m/s when there is no water; 2m/s when moving with the current and 1m/s when moving against the current when the water level ≤ 0.3m; no wading when the water level > 0.3m). The physical strength of miners is not considered, and there is a one-minute waiting time after receiving the message (the initial escape time is 60s). If the miner's or exit/entrance position is not on the roadway endpoint (e.g., some miners' positions), the projection point on the nearest roadway can be calculated using the "perpendicular distance from a point to a line segment formula", and the projection point is used as the starting point (miner) or ending point (exit/entrance) of the path to ensure that the starting and ending points of the path search are on the roadway network nodes[16].

Define: $T_{Arrival}$ (miner's arrival time at the roadway), $t_{Arrival}$ (water flow arrival time), $t_{Blockage}$ (roadway blockage time), $T_{Passage}$ (miner's passage time through the roadway).

Model Solution

To solve the problem of miners' passage time in the roadway and selecting the shortest escape time under the passage time, a two-layer model needs to be constructed. The former uses dynamic passage time

calculation modeling (combining the miner's arrival time at the roadway with the water flow state), and the latter uses the time-expanded Dijkstra algorithm to realize dynamic path exploration.

There are three scenarios for the calculation of dynamic passage time:

Scenario 1: No water in the roadway when the miner arrives ($T_{Arrival}<t_{Arrival}$)

When there is no water, the passage speed is the speed without water: $T_{Passage\ ij}=L_{ij}/V_0$

where $T_{Passage\ ij}$ represents the time taken for the miner to pass through the roadway ij.

Note: During verification, it is necessary to ensure that the miner's passage time ($T_{Arrival}+T_{Passage}$) ≤ $t_{Blockage}$. If it exceeds this, the roadway is impassable. Although there is no water now, the water flow will block the roadway before the miner leaves.

Scenario 2: There is water in the roadway when the miner arrives and the water level ≤ 0.3m ($t_{Arrival}\leq T_{Arrival}<t_{Blockage}$).

First, determine whether the miner's movement direction is consistent with the water flow direction. The water flow direction is from the endpoint where the water flow arrives first to the endpoint where it arrives later.

$$T_{Passage\ ij}=L_{ij}/V_{With\ Current} \quad \text{(With current)} \tag{7}$$

$$T_{Passage\ ij}=L_{ij}/V_{Against\ Current} \quad \text{(Against current)} \tag{8}$$

Scenario 3: The roadway is blocked when the miner arrives ($T_{Arrival}>t_{Blockage}$)

At this time, the water level in the roadway exceeds 0.3m, so wading is not recommended, and the passage time is recorded as ∞ ("impassable") (the roadway is not included in the path).

Next, the time-expanded Dijkstra algorithm is used to explore the path[17,18].

With the minimum escape time as the overall goal, the path search is performed through the time-expanded Dijkstra algorithm.

(1) First, initialize the data:

Let the initial position node of the miner be I, the initial escape time be St (60s), the arrival time of other nodes be ∞. A priority queue pq needs to be constructed, with the initial element [(St, I)] (node arrival time, current node) to store the nodes to be processed and their arrival times. Then, a predecessor node dictionary K is created to record the complete traceback route (e.g., $K_{[j]}=i$ indicates that the previous node of j is i).

(2) Iterative processing:

Each time, the node with the smallest arrival time ($(t_{\text{Node Arrival}},i)$) is popped from the queue. If the arrival time of the i-th roadway is greater than the currently recorded node arrival time (redundant data), it is skipped. It is necessary to traverse all adjacent nodes j from node i, call the function in the program, and calculate the passage time from i to j. If the time is valid (non-none indicates passable), calculate the new arrival time of j:

$$t_{\text{New Arrival Time of j}}=t_{\text{Arrival Time of i}}+T_{\text{Passage}} \tag{9}$$

If the new arrival time of j is smaller than the previously recorded arrival time of j, it indicates that an optimal path has been found, update it, and add (New Arrival Time of j, j) to the queue[19,20].

(3) Termination condition:

When the popped node i is an exit node, stop the iteration and trace back the path through the predecessor dictionary K. If no exit is found when the queue is empty, return "no feasible path".

Python code is used to draw the escape routes of workers in the two mine networks, as shown in Figures 5-6 below:

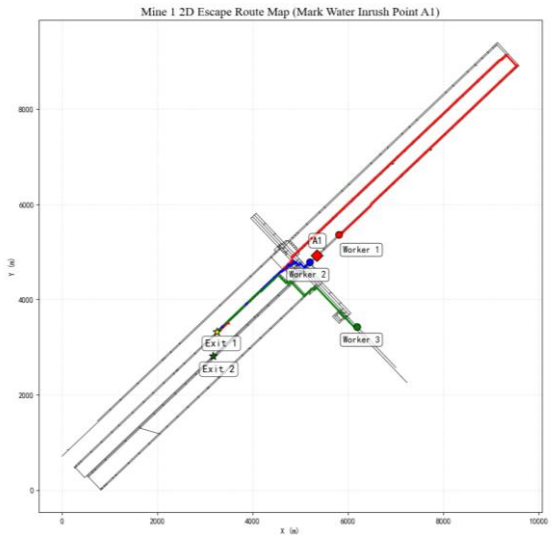

Figure 5. Worker escape routes in the mine

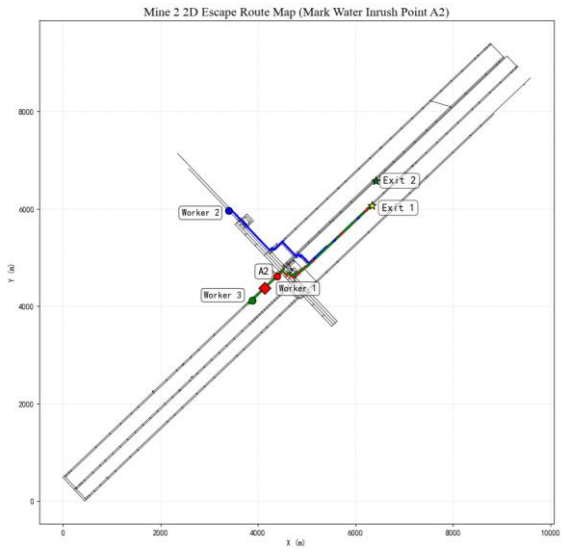

Figure 6. Worker escape routes in the mine

Model Verification

Miners' movement speeds in different roadway scenarios comply with the rules of "no water, with current/against current, impassable". The blockage time is derived based on physical constraints. For example, for a certain roadway, $t_{Arrival}=850$ s , $T_{Arrival}=620$ s , $T_{Passage}=210$ s , and $T_{Arrival}+T_{Passage}=830$ s<850 s, with a safety margin of 20s, so the verification is passed.

Integration and Superposition of Water Flow Spread Models for Dual Water Inrush Points

Model Idea and Analysis

The roadway networks are still abstracted into nodes (roadway endpoints and water inrush points) and edges as roadway lengths, and the corresponding parameters are confirmed. Determine the roadways where the water inrush points (A1, A2, B1, B2) are located. If the perpendicular distance from the water inrush point to the line connecting the endpoints is < 2m, it is within the roadway, which meets the physical premise of the water inrush point. The coordinates of the water inrush points are given in the problem, and the roadway where each water inrush point is located and the perpendicular distance can be obtained through the following formula:

$$d=\frac{|(x_i-x_j)(y_i-y_0)-(y_i-y_j)(x_i-x_0)|}{\sqrt{[(x_j-x_i)^2+(y_j-y_i)^2]}} \quad (10)$$

where (x_0,y_0) are the coordinates of the water inrush point, and (x_i,y_i), (x_j,y_j) are the coordinates of the two endpoints of the roadway.

After calculation, all water inrush points meet the requirement.

The following indicators will be used:

First arrival time at the endpoint ($t_{\text{Endpoint Arrival}}$): The time when the water flow first flows through the roadway endpoint.

First arrival time at the roadway ($t_{\text{Roadway Arrival}}$): The time when the water flow first flows through the roadway (taking the minimum of the first arrival times at the two endpoints of the roadway).

Roadway flow rate ($Q_{\text{Total Flow of Dual Sources}}$): The water volume flowing through the roadway per unit time (the total flow after superposition of dual water inrush points).

Roadway full time (t_{Full}): The time when the water level reaches the highest point of the roadway (height $l_1=3$ m).

Water flow coverage ratio: The ratio of the total length of roadways with propagated water flow to the total length of the mine network roadways.

Model Solution

Taking the data as an example, the solution is carried out in the following four steps:

Calculation of initial water flow arrival time

(1) First arrival time of water flow at the endpoint for a single water inrush point:

Let the distances from the water inrush point to the two endpoints of the initial roadway be d_i and d_j respectively:

$$t_{\text{Arrival i}}=t_{\text{Inrush}}+\frac{d_i}{v_0},\ t_{\text{Arrival j}}=t_{\text{Inrush}}+\frac{d_j}{v_0} \quad (11)$$

where t_{Inrush} is the inrush time of the water inrush point (0min for A1 and A2, 4min for B1, 5min for B2), and v_0 is the propagation speed of the water flow front.

(2) Increment of arrival time at downstream endpoints:

At branching points, the model initially assumes flow distribution as '50% horizontal, 50% downward.' This setting serves as an initial logical simplification for the baseline model, aiming to quantify the impact of height constraints. Future research should incorporate precise distribution logic based on hydraulic resistance.

For the node i whose arrival time has been calculated, the minimum arrival time of its downstream node j ($z_i \geq z_j$) is:

$$t_{min}=\min(t_{\text{Existing Time}},t_i+L_{ij}/v_0) \quad (12)$$

where L_{ij} is the length of the roadway i-j, and $t_{\text{Existing Time}}$ is the existing arrival time of node j (initially ∞).

Calculation of flow distribution (analyzed on a case-by-case basis)

(1) Roadway grouping

For the downstream roadways of node i, they are divided into horizontal roadways ($z_j=z_i$, denoted as H_{out}) and downward roadways ($z_j<z_i$, denoted as D_{out}) according to elevation. The incoming flow Q_{in} is first grouped by "50% for horizontal and 50% for downward":

$$Q_H=Q_{in}/2,\ Q_D=Q_{in}/2 \quad (13)$$

If only one type of roadway exists, the entire incoming flow is allocated to that category.

(2) Single roadway flow rate

Each roadway in the downward or horizontal group evenly divides the flow of the group:

$$Q_{ij}=Q_H/n_H \text{ (horizontal roadways)},\ Q_{ij}=Q_D/n_D \text{ (downward roadways)}$$

where n_H and n_D are the numbers of horizontal and downward roadways respectively.

Superposition of propagation results of dual water inrush points

Superposition of arrival times:

For the same endpoint, take the minimum of the arrival times of the two water inrush points (A and B, including delay):

$$t_{AB}=\min(t_A,t_B+\text{Delay Time}) \quad (14)$$

Superposition of flow rates:

For the same roadway, the total flow rate is the sum of the flow rates allocated by source A and source B:

$$Q_{\text{Total Flow of Dual Sources}}=Q_A+Q_B \quad (15)$$

Calculation of roadway full time (t_{Full}):

Roadway full time = Water flow arrival time + Time required to fill the roadway. The mathematical formula is:

$$V_{Full}=S_{Full}\times L=12L \quad (16)$$

$$t_{Full}=t_{\text{Roadway Arrival}}+(V_{Full}/Q_{\text{Total Flow of Dual Sources}}) \quad (17)$$

where V_{Full} is the volume of the roadway, and Q_{Total} is the total flow rate of the roadway.

Model Verification

The obtained data is input into the table. From the problem constraints, it can be verified that the Z-axis of all downstream nodes calculated is 10.00cm, and there are no upward or downward waterways, which does not deviate from the roadway and conforms to the problem. From the logical verification perspective, the arrival times of downstream nodes of water flow propagation are all greater than those of upstream nodes. Python software is used to generate 2D top views of Annex 1 and Annex 2, including the positions of the two water inrush points, as shown in the figure 7:

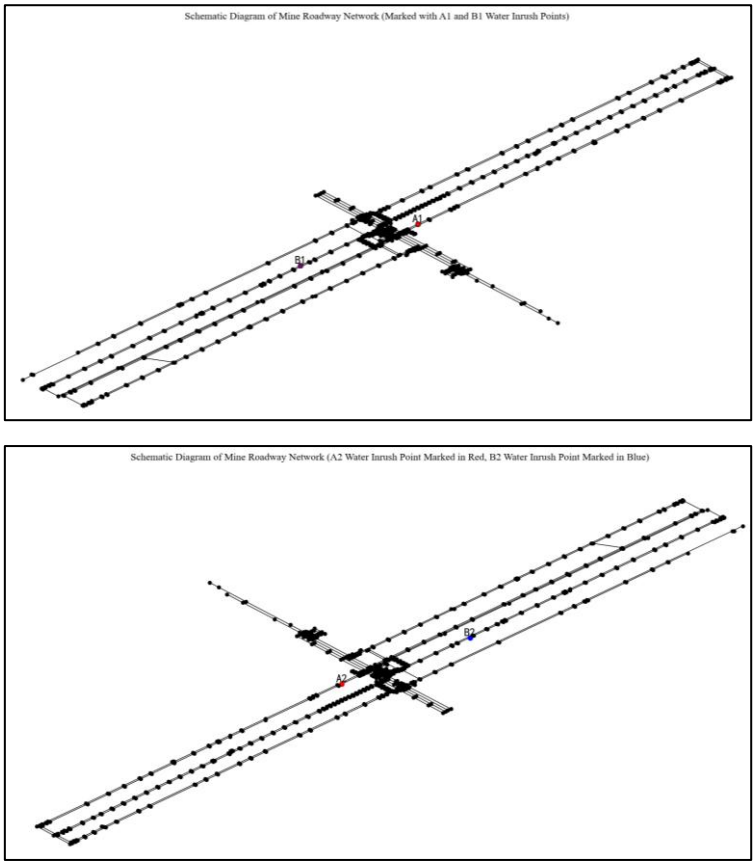

Figure 7. 2D top view (including dual water inrush points)

Optimization of Dynamic Miner Escape Paths Under Dual Water Inrush Point Conditions

Model Idea and Analysis

Based on the multi-source endpoint arrival times and roadway full times , the second water inrush point erupts with a delay, and workers are notified to evacuate one minute after the eruption. A shortest-time escape model under a time-varying road network is established:

The starting time of the water inrush point is:

$$\mathrm{St}=0\ (\mathrm{min})\ (\text{Inrush time of A1 and A2}) \tag{18}$$

The inrush time of T_B ($T_{B1}=4$; $T_{B2}=5$) (for B1/B2):

$$T_B=\text{Inrush time of the second water inrush point} \tag{19}$$

It is used to calibrate the starting point of the time axis, consistent with the time benchmark of the water flow model.

Notification release time:

$$T_{Notify}=T_B+1 \quad (20)$$

$T_{Notify1}=5$; $T_{Notify2}=6$.

The time when the notification is released one minute after the second water inrush point erupts is the starting time for miners to move.

Initial positions of miners:

$$M_k=(x_{Mk},y_{Mk},z_{Mk})\ (k=1,2,3) \quad (21)$$

Coordinates of the j-th exit/entrance are the endpoints of the escape path.

Set of all roadways in the mine:

$$LL=\{L_1,L_2,...,L_m\} \quad (22)$$

Each roadway L connects endpoints u_L and v_L, with length:

$$L_L=\sqrt{(x_{u_L}-x_{v_L})^2+(y_{u_L}-y_{v_L})^2+(z_{u_L}-z_{v_L})^2}\ \text{(Euclidean distance)} \quad (23)$$

The direction of the roadway is defined based on the elevation difference of the endpoints, pointing from the endpoint with higher elevation to the endpoint with lower elevation. That is, if $z_i>z_j$, the direction of the roadway is from i to j. This direction rule is consistent with the natural flow law of water flow, providing a basis for subsequent determination of the passage direction.

Model Solution

Calculation of dynamic passage time

The first arrival time $t_{Arrival}$ of the endpoint and the full time t_{Full} are used to construct a piecewise function $h_l(t)$ of the water depth changing with time for each roadway l. It is agreed that during the period from the first arrival of the water flow to the full state ($t_{Arrival} \leq t \leq t_{Full}$), the water depth is calculated as linear elevation; if the roadway is never full ($t > t_{Full}$ or there is no full time), the water depth remains at the maximum value $h_{l,max}$. The formula is expressed as:

$$h_l(t) = \begin{cases} 0, & t << t_{Arrival} \\ \dfrac{h_{l,max}}{t_{Full} - t_{Arrival}} (t - t_{Arrival}), & t_{Arrival} \leq t \leq t_{Full} \\ h_{l,max}, & t > t_{Full} \end{cases} \quad (24)$$

This function strictly follows the safety rule of "impassable when the water depth exceeds 0.3m". When $h_l(t) \geq 0.3$ m, the roadway is impassable. Based on the time-expanded Dijkstra algorithm, and considering the fusion of dual water inrush points, the escape paths of miners under dual water inrush points can be obtained with Python. The following figures (Figure 8 and Figure 9) show the escape path diagrams of 6 miners:

It can be seen from the figure 8 that since workers start to evacuate one minute after the B1 water inrush point erupts, the A1 water inrush point has been continuously erupting for five minutes at this time. Among them, Worker 1 is not only the farthest from the exit but also extremely close to the water inrush point. The water levels at the key nodes on his escape route have all exceeded 0.3 meters. According to the problem settings, Worker 1 failed to escape successfully.

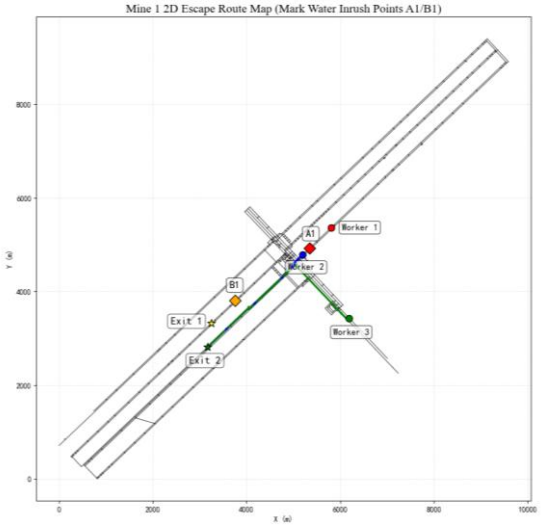

Figure 8. Worker escape path diagram in the mine under dual water inrush points

The figure 9 above shows that all 3 miners in the mine escaped successfully.

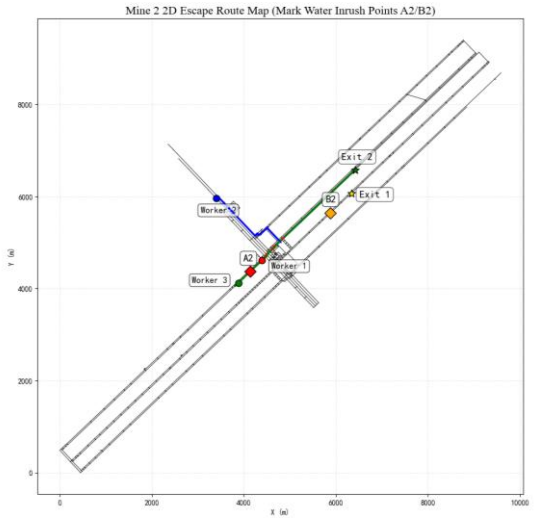

Figure 9. Worker escape path diagram in the mine under dual water inrush points (marked with water inrush points A2/B2)

CONCLUSIONS

This study develops a model for predicting water flow propagation in mine tunnel water inrushes and planning dynamic miner escape routes, simulating single-source and delayed dual-source scenarios. For flow prediction, a roadway network graph is built using tunnel endpoints and water inrush points, with the BFS algorithm calculating water arrival and flooding times based on parameters like roadway dimensions (width 4m, height 3m) and water volume (30m³/s). The model highlights elevation constraints on flow distribution and identifies topologically safe zones. For escape planning, miner speed (4 m/s dry, prohibited at water depth >0.3 m) is converted to dynamic travel times, using a time-extended Dijkstra algorithm for shortest paths. These quantitative results provide practical references for the optimized design of industrial textiles used in mine-rescue gear, ensuring that the equipment supports the evacuation mobility requirements identified in this study. Dual-source inrushes are modeled via time-axis shifting, flow superposition, and defining evacuation start as “one minute after the second inrush,” with path feasibility validated by piecewise water depth functions.

Limitations and Future Research

The current model simplifies the relationship between human movement speed and water depth using a piecewise linear approximation. This overlooks the nonlinear effects of resistance and buoyancy on

underwater motion. Future work should refine the motion model by incorporating human biomechanical parameters. This model currently employs linear calculations based on geometric distance and constant flow velocity to determine the arrival time of water inflow. It does not yet fully account for the complex hydrodynamic characteristics in underground tunnels, such as friction losses, turbulence, and the influence of time-varying pressure heads on flow velocity. The model simplifies water inrush and evacuation processes. It assumes miner speed depends only on water depth and flow direction, ignoring crowd congestion, psychological factors, and emergency inefficiencies. In high-density scenarios, shortest-time paths may not be safest. Roadway simulation uses “end-point centerlines,” overlooking curvature, variable cross-sections, and storage effects. Future work should integrate crowd dynamics for safer path planning in dense conditions and refine hydrodynamic models or parameterize tunnel storage for better accuracy in complex geometries and localized water regulation. Additionally, future work could explore the integration of flexible textile-based sensors into the proposed dynamic system to provide real-time data for precise path recalibration.

Author Contributions

Conceptualization –Deng J, Li W, Liu SJ and Wang ST; methodology – Deng J, Li W and Wang ST; model construction – Deng J and Li W; literature review – Liu SJ and Wang ST; writing-original draft preparation – Liu SJ and Wang ST; writing-review and editing – Deng J, Liu SJ and Wang ST; model solution, data analysis and visualization – Li W; supervision – Deng J. All authors have read and agreed to the published version of the manuscript.

Conflicts of Interest

The authors declare no conflict of interest.

Funding

This research was funded by the 2023 annual project of the 14th Five-Year Plan of Changsha Education Science, grant number CJK2023103.

Acknowledgements

Thanks to all the members for their efforts.

REFERENCES

[1] Guzy A. Environmental Impacts of Post-Closure Mine Flooding: An Integrated Remote Sensing and Geospatial Analysis of the Olkusz-Pomorzany Mine, Poland. Water. 2025; 17(23):3337-3337. doi: 10.3390/W17233337

[2] Mohammadi MA. Dynamic Simulation and Conceptual Interaction Between Groundwater Level, Groundwater Pumping Costs, and Land Uplift in Abandoned Coal Mines in Germany.Mining, Metallurgy & Exploration. 2025; 42(5):1-24. doi: 10.1007/S42461-025-01338-6

[3] Desmau M, Skierszkan KE, Oka G, Kaur I, Schoepfer VA, Flather D, et al. Multi-contaminant removal from synthetic mine-impacted water by permeable reactive barriers under cold conditions..Chemosphere. 2025; 384:144499. doi: 10.1016/J.CHEMOSPHERE.2025.144499

[4] Miclean M, Cadar O, Muntean A, Levei L. Mine Water Discharge Chemistry and Potential Risk in a Former Mining Area.Environments. 2025; 12(3):76-76. doi: 10.3390/ENVIRONMENTS12030076

[5] Marmier V, Plante B, Demers I, Benzaazoua M. Neutral Mine Drainage prediction for different waste rock lithologies–Case study of Canadian Malartic. Journal of Geochemical Exploration. 2025; 271:107685-107685. doi: 10.1016/J.GEXPLO.2025.107685

[6] Misa R, Sroka A, Mrocheń D. Evaluating Surface Stability for Sustainable Development Following Cessation of Mining Exploitation.Sustainability. 2025; 17(3):878-878. doi: 10.3390/SU17030878

[7] Li B, Wu H, Wu Q, Zeng Y, Guo X. Prediction technology of mine water inflow based on entropy weight method and multiple nonlinear regression theory and its application.Geomechanics and Geophysics for Geo-Energy and Geo-Resources. 2024; 10(1):127-127. doi: 10.1007/S40948-024-00842-1

[8] Rudakov D, Sun Y, Inkin O. Optimization of mine water discharge with the river hydrograph. Case study Samara River in Western Donbas. IOP Conference Series: Earth and Environmental Science. 2024; 1348(1). doi: 10.1088/1755-1315/1348/1/012041

[9] Quandt D, Busch B, Greve J, Hilgers C. Rock characteristics and reservoir properties of Upper Carboniferous (Stephanian A–B) tight siliciclastic rocks from the Saar–Nahe basin (SW Germany). International Journal of Earth Sciences. 2024; 113(8):1-23. doi: 10.1007/S00531-024-02394-X

[10] Mugova E, Molaba L, Wolkersdorfer C. Understanding the Mechanisms and Implications of the First Flush in Mine Pools: Insights from Field Studies in Europe's Deepest Metal Mine and Analogue Modelling. Mine Water and the Environment. 2024; 43(1):73-86. doi: 10.1007/S10230-024-00969-3

[11] Yao D, Chen S, Dong S, Qin J. Modeling abrupt changes in mine water inflow trends: A CEEMDAN-based multi-model prediction approach. Journal of Cleaner Production. 2024; 439:140809. doi: 10.1016/J.JCLEPRO.2024.140809

[12] Yan P, Li G, Wang W, Zhao Y, Wang J, Wen Z. A Mine Water SAource Prediction Model Based on LIF Technology and BWO-ELM. Journal of fluorescence. 2024; 35(2):1-16. doi: 10.1007/S10895-023-03575-8

[13] Zhai H, Wang J, Lu Y, Rao Z, He K, Hao S, et al. Prediction of the Mine Water Inflow of Coal-Bearing Rock Series Based on Well Group Pumping. Water. 2023; 15(20):3680. doi: 10.3390/W15203680

[14] Rybnikova LS, Rybnikov PA, Smirnov AY. Post-mining of Chelyabinsk Coal Basin (Russia): The Effects of Mine Flooding. Mine Water and the Environment. 2023; 42(3):472-488. doi: 10.1007/S10230-023-00947-1

[15] Ovchinnikov NP, Zyryanov IV. Impact of Increased Water Inflow on Main Drainage System Efficiency in Mine. Journal of Mining Science. 2023; 59(2):342-347. doi: 10.1134/S1062739123020175

[16] Zhang B, Li F, Zhang M, Yu Z, Wang X. Evaluation of mine water inflow quality based on multiple methods. Journal of Environmental Engineering and Science. 2023; 18(4):215-225. doi: 10.1680/JENES.23.00036

[17] Li B, Wu H, Liu P, Fan J, Li T. Construction and application of mine water inflow prediction model based on multi-factor weighted regression: Wulunshan Coal Mine case. Earth Science Informatics. 2023; 16(2):1879-1890. doi: 10.1007/S12145-023-00985-X

[18] Yang S, Lian H, Xu B, Thanh HV, Chen W, Yin H, et al. Application of robust deep learning models to predict mine water inflow: Implication for groundwater environment management. Science of the Total Environment. 2023; 871:162056-162056. doi: 10.1016/J.SCITOTENV.2023.162056

[19] Merkulova V, Tretyakova Z, Evtushenko A. Environmental safety model of the region in conditions of large-scale mine liquidation. E3S Web of Conferences. 2023; 371. doi: 10.1051/E3SCONF/202337106023

[20] Rische M, Fischer KD, Friederich W. FloodRisk–Induced seismicity by mine flooding–Observation, characterisation and relation to mine water rise in the eastern Ruhr area (Germany). Zeitschrift der Deutschen Gesellschaft für Geowissenschaften. 2022; 173(4):551-564. doi: 10.1127/ZDGG/2023/0346